Stimulus-Responsive Poly(*N*-isopropylacrylamide) Brushes and Nanopatterns Prepared by Surface-Initiated Polymerization

Marian Kaholek,[†,‡] Woo-Kyung Lee,[†,‡] Sang-Jung Ahn,[§] Hongwei Ma,[∥] Kenneth C. Caster,[‡] Bruce LaMattina,[⊥,‡] and Stefan Zauscher*[,†,‡]

Department of Mechanical Engineering and Materials Science, 144 Hudson Hall, Box 90300, Duke University, Durham, North Carolina 27708-0300, Center for Biologically Inspired Materials and Material Systems, Duke University, Durham, North Carolina 27708-0303, Department of Computer Science, Duke University, Durham, North Carolina 27708-0129, Department of Biomedical Engineering, Duke University, Durham, North Carolina 27708-0281, and Army Research Office, P.O. Box 12211, Research Triangle Park, North Carolina 27709-2211

Received March 16, 2004. Revised Manuscript Received July 12, 2004

In this paper we report the surface-initiated polymerization of poly(*N*-isopropylacrylamide) (pNIPAAM), a stimulus-responsive polymer, from monolayers of ω-mercaptoundecyl bromoisobutyrate on gold-coated surfaces. pNIPAAM was polymerized in aqueous solution at a low methanol concentration at room temperature to maintain the growing pNIPAAM chains in a hydrophilic and an extended conformational state. Under these conditions thick polymer brush layers (up to 500 nm in the swollen state) are produced after 1 h of polymerization. We present a new and simple strategy to fabricate stimulus-responsive, surface-confined pNIPAAM brush nanopatterns prepared in a "grafting-from" approach that combines "nanoshaving", a scanning probe lithography method, with surface-initiated polymerization. The reversible, stimulus-responsive conformational height change of bulk and nanopatterned polymer brushes was demonstrated by repeated cycling in water and water/methanol mixtures (1:1, v/v). Our findings are consistent with the behavior of laterally confined and covalently attached polymer chains, where chain mobility is restricted largely to the out-of-plane direction. The present work is significant because the triggered control of interfacial properties on the nanometer scale holds significant promise for actuation in bio-nanotechnology applications where polymeric actuators may manipulate the transport, separation, and detection of biomolecules.

Introduction

One central goal of materials engineering on the nanometer and micrometer length scales is to produce materials that are ordered over a range of length scales and in which larger scale structural and physicochemical properties are controlled by molecular characteristics.[1] For example, growing polymer brushes with thicknesses on the molecular scale from solid surfaces allows one to tailor the surface properties of materials by imparting desirable energetic, mechanical, and electrical functionalities.[2] The in situ formation of dense polymer brushes is possible through a "grafting-from" approach[3] in which covalently attached polymers are grown by surface-initiated polymerization from the substrate, yielding larger packing densities than those prepared in a "grafting-to" approach that seeks to direct macromolecules to a surface and immobilize them there.

Although the templated fabrication of polymer brushes has been prototypically demonstrated, and many methods to initiate polymerization reactions have been used (e.g., anion,[4] cation,[5,6] radical,[3] plasma,[7] condensation,[8] photochemical,[9,10] electrochemical,[11] and ring-opening metathesis[12,13] polymerization), fabrication of precisely patterned, surface-attached polymeric nanostructures with controlled chain lengths, chemical functionality, shape, and feature dimensions is still in its infancy.

* To whom correspondence should be addressed. Phone: (919) 660-5360. Fax: (919) 660-8963. E-mail: zauscher@duke.edu.
[†] Department of Mechanical Engineering and Materials Science, Duke University.
[‡] Center for Biologically Inspired Materials and Material Systems, Duke University.
[§] Department of Computer Science, Duke University.
[∥] Department of Biomedical Engineering, Duke University.
[⊥] Army Research Office.

(1) Dan, N. *Trends Biotechnol.* **2000**, *18*, 370−374.
(2) Zhao, B.; Brittain, W. J. *Prog. Polym. Sci.* **2000**, *25*, 677−710.
(3) Prucker, O.; Rühe, J. *Macromolecules* **1998**, *31*, 592−601.
(4) Jordan, R.; Ulman, A.; Kang, J. F.; Rafailovich, M. H.; Sokolov, J. *J. Am. Chem. Soc.* **1999**, *121*, 1016−1022.
(5) Jordan, R.; Ulman, A. *J. Am. Chem. Soc.* **1998**, *120*, 243−247.
(6) Zhao, B.; Brittain, W. J. *J. Am. Chem. Soc.* **1999**, *121*, 3557−3558.
(7) Chen, W.; Fadeev, A. Y.; Hsieh, M. C.; Oner, D.; Youngblood, J.; McCarthy, T. J. *Langmuir* **1999**, *15*, 3395−3399.
(8) Husemann, M.; Mecerreyes, D.; Hawker, C. J.; Hedrick, J. L.; Shah, R.; Abbott, N. L. *Angew. Chem., Int. Ed.* **1999**, *38*, 647−649.
(9) Prucker, O.; Naumann, C. A.; Rühe, J.; Knoll, W.; Frank, C. W. *J. Am. Chem. Soc.* **1999**, *121*, 8766−8770.
(10) Lee, H. J.; Nakayama, Y.; Matsuda, T. *Macromolecules* **1999**, *32*, 6989−6995.
(11) Gurtner, C.; Wun, A. W.; Sailor, M. *Angew. Chem., Int. Ed.* **1999**, *38*, 1966−1968.

10.1021/cm049562y CCC: $27.50
Published on Web 08/27/2004

Several studies explored micro- and nanofabrication of polymeric structures in a grafting-from approach using microcontact printing,[8,13−16] photolithography,[17] chemical lithography,[18] contact molding,[19] scanning probe lithography (SPL),[20−24] electron-beam lithography,[25] multiphoton fabrication by a femtosecond laser,[26] and chromium-patterned silicon wafers.[27]

Atom-transfer radical polymerization[28] (ATRP) has been the polymerization methodology used most extensively by researchers attempting to prepare surface-attached polymer brushes of controlled structure. This transition-metal-based, controlled radical polymerization chemistry produces functional polymers with defined molecular weight and polydispersity and, as a result of the "living" nature of the initiator, allows the ready synthesis of block copolymers. ATRP has also been applied to polymerize *N*-isopropylacrylamide (NIPAAM).[29,30]

Poly(*N*-isopropylacrylamide) (pNIPAAM) is a stimulus-responsive polymer that undergoes a reversible, inverse phase transition at a lower critical solution temperature (LCST) of about 32 °C in pure water.[31] In addition to temperature, cosolvents can also cause an inverse phase transition in pNIPAAM. For example, the addition of 50% methanol by volume to aqueous pNIPAAM solutions leads to co-nonsolvency,[32,33] effectively lowering the LCST of pNIPAAM to below 0 °C.

The functionality of pNIPAAM on surfaces can be separated into two categories: (1) triggered changes in polymer conformation and (2) triggered changes in polymer surface energetics. Below the LCST, pNIPAAM is hydrated and the chains are in an extended conformational state. Above the LCST, pNIPAAM is in a hydrophobically collapsed conformational state. Polymer brushes with triggerable phase transition behavior, such as pNIPAAM, can be exploited in devices on the nano- and microscales, with potential applications for protein affinity separations[34] and in micro- and nanofluidics.[35]

Here we report the surface-initiated polymerization of pNIPAAM from monolayers of the thiol initiator ω-mercaptoundecyl bromoisobutyrate (**1**) on gold-coated surfaces where the growing pNIPAAM chains are in a hydrophilic and extended conformational state, yielding a thick polymer brush layer. To fabricate surface-confined pNIPAAM brush nanopatterns prepared in a grafting-from approach, we have developed a novel method[24] that combines "nanoshaving",[36] an SPL method, with surface-initiated polymerization.

Materials and Methods

Materials. NIPAAM (97%) monomer, copper(I) bromide (Cu^IBr; 99.9%), 1-octadecanethiol (ODT; 98%), and methanol (MeOH; 99.9%) were obtained from Sigma-Aldrich (Milwaukee, WI). NIPAAM was purified by recrystallization from toluene/hexane before use. Milli-Q (Millipore, Billerica, MA) water (18 MΩ/cm) and methanol were used as polymerization solvents. *N*,*N*,*N*′,*N*″,*N*″-Pentamethyldiethylenetriamine (PMDETA) was used as received from Acros Organics (Hampton, NH).

Methods. *Preparation of Substrates.* To immobilize the initiators for surface-initiated polymerization, gold substrates with an average grain diameter of 30 nm were prepared by thermal evaporation under a vacuum of 4×10^{-7} Torr. For this purpose an adhesion layer of chromium (50 Å) followed by a layer of gold (500 Å) was evaporated onto silicon wafers. For interaction force measurements the underside of atomic force microscopy (AFM) silicon nitride (Si_3N_4) cantilevers (Nanoprobe, Veeco, Santa Barbara, CA; spring constant 0.12 N/m) was coated by the same process. Before deposition, silicon wafers and AFM cantilevers were cleaned in a mixture of H_2O_2/H_2SO_4 (1:3, v/v) at 80 °C ("piranha solution") for 10 min and washed thoroughly with Milli-Q-grade water. *(Caution: Piranha solution reacts violently with organic matter!)*

Preparation of Initiator Monolayers. The thiol initiator **1** ($BrC(CH_3)_2COO(CH_2)_{11}SH$) was synthesized as reported.[37] A self-assembled monolayer (SAM) of the thiol initiator **1** was obtained by immersing clean, gold-coated Si substrates and gold-coated AFM cantilevers in a 1 mM ethanolic solution of the thiol initiator for 1 day. After incubation, the substrates and cantilevers were washed with copious amounts of ethanol, sonicated in ethanol for 1 min (except for cantilevers), and then rinsed again in ethanol to remove the excess of thiols. The samples were finally dried in a stream of dry nitrogen and immediately transferred into the polymerization solution.

Nanopatterning of the Thiol Initiator. A SAM of ODT, forming a hydrophobic resist layer on gold-coated silicon substrates, was prepared by immersion of substrates in a 1 mM ethanolic solution of ODT for 48 h. The ODT SAM was patterned by nanoshaving,[36] i.e, by directed mechanical ablation of the ODT resist using an atomic force microscope where a silicon nitride (Si_3N_4) AFM cantilever (Nanoprobe, Veeco; spring constant 0.12 N/m; tip radius 20−60 nm) was used in contact mode. We applied large normal forces (∼50 nN) and high scan speeds (∼20 μm/s) to remove the resist and create a pattern of straight "trenches" on the substrate surface. A Hertzian contact mechanics analysis[38] reveals that the applied maximal stress beneath the AFM tip exceeds the yield stress

(12) Weck, M.; Jackiw, J. J.; Rossi, R. R.; Weiss, P. S.; Grubbs, R. H. *J. Am. Chem. Soc.* **1999**, *121*, 4088−4089.
(13) Jeon, N. L.; Choi, I. S.; Whitesides, G. M.; Kim, N. Y.; Laibinis, P. E.; Harada, Y.; Finnie, K. R.; Girolami, G. S.; Nuzzo, R. G. *Appl. Phys. Lett.* **1999**, *75*, 4201−4203.
(14) Jones, D. M.; Huck, W. T. S. *Adv. Mater.* **2001**, *13*, 1256−1259.
(15) Hyun, J.; Chilkoti, A. *Macromolecules* **2001**, *34*, 5644−5652.
(16) Guo, W. F.; Jennings, G. K. *Adv. Mater.* **2003**, *15*, 588−591.
(17) Prucker, O.; Schimmel, M.; Tovar, G.; Knoll, W.; Rühe, J. *Adv. Mater.* **1998**, *10*, 1073−1077.
(18) Schmelmer, U.; Jordan, R.; Geyer, W.; Eck, W.; Golzhauser, A.; Grunze, M.; Ulman, A. *Angew. Chem., Int. Ed.* **2003**, *42*, 559−563.
(19) von Werne, T. A.; Germack, D. S.; Hagberg, E. C.; Sheares, V. V.; Hawker, C. J.; Carter, K. R. *J. Am. Chem. Soc.* **2003**, *125*, 3831−3838.
(20) Liu, X.; Guo, S.; Mirkin, C. A. *Angew. Chem., Int. Ed.* **2003**, *42*, 4785−4789.
(21) Maynor, B. W.; Filocamo, S. F.; Grinstaff, M. W.; Liu, J. *J. Am. Chem. Soc.* **2002**, *124*, 522−523.
(22) Okawa, Y.; Aono, M. *Nature* **2001**, *409*, 683−684.
(23) Jahromi, S.; Dijkstra, J.; van der Vegte, E.; Mostert, B. *ChemPhysChem* **2002**, *3*, 693−696.
(24) Kaholek, M.; Lee, W. K.; LaMattina, B.; Caster, K. C.; Zauscher, S. *Nano Lett.* **2004**, *4*, 373−376.
(25) Tsujii, Y.; Ejaz, M.; Yamamoto, S.; Fukuda, T.; Shigeto, K.; Mibu, K.; Shinjo, T. *Polymer* **2002**, *43*, 3837−3841.
(26) Campagnola, P. J.; Delguidice, D. M.; Epling, G. A.; Hoffacker, K. D.; Howell, A. R.; Pitts, J. D.; Goodman, S. L. *Macromolecules* **2000**, *33*, 1511−1513.
(27) de Boer, B.; Simon, H. K.; Werts, M. P. L.; van der Vegte, E. W.; Hadziioannou, G. *Macromolecules* **2000**, *33*, 349−356.
(28) Matyjaszewski, K.; Xia, J. H. *Chem. Rev.* **2001**, *101*, 2921−2990.
(29) Jones, D. M.; Smith, J. R.; Huck, W. T. S.; Alexander, C. *Adv. Mater.* **2002**, *14*, 1130−1134.
(30) Balamurugan, S.; Mendez, S.; Balamurugan, S. S.; O'Brien, M. J.; Lopez, G. P. *Langmuir* **2003**, *19*, 2545−2549.
(31) Schild, H. G. *Prog. Polym. Sci.* **1992**, *17*, 163−249.
(32) Winnik, F. M.; Ringsdorf, H.; Venzmer, J. *Macromolecules* **1990**, *23*, 2415−2416.
(33) Schild, H. G.; Muthukumar, M.; Tirrell, D. A. *Macromolecules* **1991**, *24*, 948−952.
(34) Nath, N.; Chilkoti, A. *Adv. Mater.* **2002**, *14*, 1243−1247.
(35) Beebe, D. J.; Moore, J. S.; Yu, Q.; Liu, R. H.; Kraft, M. L.; Jo, B. H.; Devadoss, C. *Proc. Natl. Acad. Sci. U.S.A.* **2000**, *97*, 13488−13493.
(36) Liu, G. Y.; Xu, S.; Qian, Y. L. *Acc. Chem. Res.* **2000**, *33*, 457−466.
(37) Jones, D. M.; Brown, A. A.; Huck, W. T. S. *Langmuir* **2002**, *18*, 1265−1269.

Scheme 1. Surface-Initiated Polymerization of NIPAAM on Gold Surfaces To Yield pNIPAAM Polymer Brushes

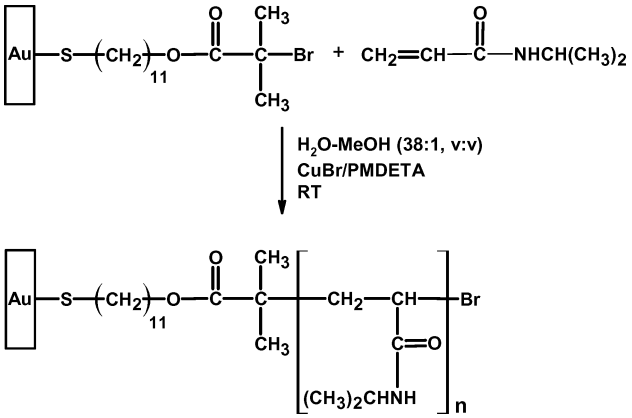

in amorphous gold thin films,[39] which suggests that the underlying gold substrate likely was plastically deformed during nanoshaving. The extent of resist removal was controlled by varying the shaving time while maintaining a constant scan speed of 20 μm/s. Subsequently, the freshly exposed gold surface in these trenches was backfilled by immersing the substrate for 30 min in a 1 mM ethanolic solution of the thiol initiator **1** to form an initiator pattern of parallel lines. The substrate was then washed with copious amounts of ethanol, sonicated in ethanol for 1 min, and rinsed again in ethanol to remove excess, loosely bound thiols. The sample was finally dried in a stream of dry nitrogen. We were unable to obtain well-defined lateral force AFM images of the patterned thiol initiator **1** because the chemical functionality of the initiator **1** was not sufficiently different from the background to cause an appreciable surface free energy change.

NIPAAM Polymerization. Scheme 1 outlines the synthetic pathway for the preparation of pNIPAAM brushes on gold surfaces by surface-initiated polymerization. In this process, gold substrates decorated with SAMs of thiol initiator **1** were immersed in the polymerization solution for a specified time period under a nitrogen atmosphere. Prior to use, all solutions and flasks were thoroughly flushed with nitrogen to remove oxygen. A monolayer film of the thiol initiator **1** was prepared by immersion of gold-coated wafers in a 1 mM ethanolic solution of the thiol initiator for 24 h. The polymerization solution was prepared by adding a solution of NIPAAM monomer to an organometallic catalyst. The organometallic catalyst was formed in a nitrogen atmosphere by adding $Cu^{I}Br$ (3.7 mg, 0.026 mmol) and PMDETA (27 μL, 0.129 mmol) in a 1:5 molar ratio to 1.5 mL of MeOH as solvent. The mixture was then sonicated for 1−2 min to facilitate the formation of the $Cu^{I}Br$/PMDETA complex. In the absence of a deactivator ($CuBr_2$), the metal complex CuBr/PMDETA served only to facilitate the initiation through a redox process, and the reaction can be considered as a redox-initiated, free radical polymerization.[40] Next, 12.5 g (110 mmol) of NIPAAM monomer dissolved in 57 mL of water (18 wt %) was filtered into the catalyst−complex solution through a 0.45 μm Millipore Millex filter. The molar ratio of NIPAAM to Cu(I) was fixed at 4300:1 at a volume ratio of MeOH to water of 1:38 for all polymerizations. The polymerization solution was then transferred into flasks containing the sample substrates with immobilized initiator. The flasks were sealed with rubber septa and kept at room temperature under nitrogen. To obtain different brush thicknesses, polymerization times were varied from 5 to 60 min without stirring. After the desired reaction time, substrates were removed from the polymerization solution, exhaustively rinsed with Milli-Q water to remove all traces of the polymerization solution, and subsequently dried in a stream of nitrogen. In ATRP, a highly reactive and, in our case, surface-tethered, organic radical is generated along with a stable Cu(II) species that can be regarded as a persistent metalloradical, which is not able to initiate radical polymerization in the polymerizing solution.[28] This means that polymerization is strictly confined to the surface-attached, growing polymer chains. As a check for the presence of polymer in solution, an aqueous polymerizing solution was poured into an equal volume of MeOH at room temperature to induce a phase transition. The absence of precipitation of polymer in the solution indicated that no polymerization had taken place in solution.

To prepare nanopatterned pNIPAAM brushes, gold substrates decorated with line patterns of thiol initiator were immersed for 60 min in a polymerization solution of the same composition as that used for the preparation of bulk polymer brushes. The pNIPAAM brushes on gold-coated AFM cantilevers were prepared by a similar procedure.

Reflectance FTIR Spectroscopy. Reflectance FTIR spectroscopy was performed using a Thermo Nicolet Nexus 670 spectrometer with an ATR (attenuated total reflectance) accessory, fitted with a nitrogen-cooled MCT detector. For each spectrum, 128 scans with a nominal resolution of 4 cm^{-1} were collected.

Ellipsometry. Ellipsometric measurements of the polymer brush thickness in water and in water/MeOH mixtures were made on a customized Rudolph Research null ellipsometer (model 43603, 200E) at a wavelength of 4015 Å.[41] The optical properties of the gold substrate and the thiol initiator layer were determined by measuring the ellipsometric angles in two different media (air and Milli-Q-grade water) using four-zone null averaging.[41] The mean refractive index and the average polymer brush thicknesss were calculated numerically from the ellipsometric angles Ψ and Δ using an optical four-layer model.[42]

Atomic Force Microscopy. The pNIPAAM brush substrates were rinsed with Milli-Q water, dried under a stream of nitrogen, and mounted on steel sample disks prior to AFM measurements. The AFM topographic images were collected in contact mode using V-shaped silicon nitride cantilevers (Nanoprobe, Veeco; spring constant 0.12 N/m; tip radius 20−60 nm) using a MultiMode atomic force microscope (Digital Instruments, Santa Barbara, CA). Topographic imaging was performed in air, in water, and in water/methanol (1:1, v/v) mixtures using a fluid cell. The AFM topographic images were collected under low applied normal forces (~1 nN) to minimize compression and lateral damage of the polymer brushes. The actual thickness of a solvated brush, in the absence of any applied imaging forces, is likely larger than the measured apparent thickness obtained from AFM contact mode imaging.[43] Patterned areas were located accurately and repeatedly by pixel correlation using still-video micrographs captured during lithography.

To measure brush thickness, samples were carefully scored with a razor blade tip, removing only the brush and Au/Cr layer.[44] Several control experiments on bare, clean silica wafers and on gold-coated silica wafers showed that it was not possible to scratch the pure silica substrate by gentle scratching while the Au/Cr layer was easily removed down to the bare silica surface. The brush thickness, B_t, was determined from cross-sectional analysis of AFM height images taken at the boundary between the scratched and nonscratched regions using eq 1,

(38) Landau, L. D.; Lifshits, E. M. *Theory of Elasticity*, 2nd ed.; Pergamon Press: Oxford, 1970.
(39) Espinosa, H. D.; Prorok, B. C. *J. Mater. Sci.* **2003**, *38*, 4125−4128.
(40) Matyjaszewski, K.; Miller, P. J.; Shukla, N.; Immaraporn, B.; Gelman, A.; Luokala, B. B.; Siclovan, T. M.; Kickelbick, G.; Vallant, T.; Hoffmann, H.; Pakula, T. *Macromolecules* **1999**, *32*, 8716−8724.
(41) Landgren, M.; Jönsson, B. *J. Phys. Chem.* **1993**, *97*, 1656−1660.
(42) Tiberg, F.; Landgren, M. *Langmuir* **1993**, *9*, 927−932.
(43) Kidoaki, S.; Ohya, S.; Nakayama, Y.; Matsuda, T. *Langmuir* **2001**, *17*, 2402−2407.
(44) Yamamoto, S.; Ejaz, M.; Tsujii, Y.; Matsumoto, M.; Fukuda, T. *Macromolecules* **2000**, *33*, 5602−5607.

where S_h is the average step height of the scratch (i.e., the combined thickness of the polymer brush and the Au/Cr layer) and G_t is the average thickness of the Au/Cr layer, measured before polymerization.

$$B_t = S_h - G_t \quad (1)$$

Surface Force Measurements. Interaction forces between pNIPAAM brushes and pNIPAAM-decorated cantilever tips were measured by AFM in force spectrometry mode (MultiMode atomic force microscope with a Nanoscope IIIa controller, Digital Instruments). The cantilever stiffness was estimated from the power spectral density of the thermal noise fluctuations.[45] The sensitivity of the photodiode detector was determined from the constant compliance regime upon approach at large applied normal force. The zero of separation was customarily chosen to coincide with the constant compliance regime. Approach and retraction rates were kept below 1 μm/s to minimize hydrodynamic drag forces, and measurements were performed in a background electrolyte concentration of 0.01 M NaCl to decrease electric double-layer interactions. To obtain good statistics, at least 20 force−distance curves were recorded at each position and measurements were repeated at several locations on the sample. To investigate the reversibility of the LCST behavior, force measurements were repeated several times, switching from water to 1:1 (v/v) water/methanol mixtures to induce the phase transition.

Results and Discussion

Surface-Initiated Bulk Polymerization. As outlined in the synthetic pathway for the preparation of pNIPAAM brushes (Scheme 1), initiator **1** monolayers were prepared by immersion of gold-coated wafers in a 1 mM ethanolic solution of the thiol initiator **1** for 24 h. Reflectance FTIR spectra show the appearance of a carbonyl peak at 1730 cm^{-1} (Figure 1a), confirming initiator immobilization on the substrate. Immersion of the substrate in an aqueous solution of NIPAAM with low MeOH content (2.6 vol %) containing the CuBr/PMDETA catalyst initiates the polymerization. The major IR absorption peaks of the resulting pNIPAAM brushes (Figure 1b) are identical to those for linear pNIPAAM polymerized in aqueous solution,[46] verifying the presence of pNIPAAM on the surface. The absorption peak at 3300 cm^{-1} in Figure 1b can be attributed to the stretch of the hydrogen-bonded NH group. The antisymmetric stretching vibration of the CH_3 group occurs at 2970 cm^{-1}, the secondary amide C═O stretching givea rise to a strong band at 1640 cm^{-1}, and the antisymmetric bending deformation of CH_3 occurs at 1460 cm^{-1}. The two bands at 1370 and 1390 cm^{-1} of almost equal intensity are assigned to the two methyl groups in the isopropyl functionality.

It is well-known that ATRP of hydrophilic monomers can be accelerated greatly in aqueous media,[47,48] and recently Huck et al.[29] demonstrated the controlled polymerization of pNIPAAM brushes with brush thicknesses up to 100 nm (dry state), from SAM-bound initiators using ATRP in a mixture of water/MeOH (1:1, v/v). Under the reaction conditions chosen by Huck et al.,[29] the pNIPAAM brush was likely formed in a hydrophobically collapsed conformational state,[32,33] which likely limits the molecular weight and brush uniformity.[49] To optimize brush growth by performing the polymerization in the conformationally extended state, we polymerized pNIPAAM in water at a low methanol concentration (2.6 vol %), as MeOH concentrations of less than 5 vol % do not affect the LCST behavior significantly.[32,33] A small amount of methanol, however, is needed to achieve good solubility of the initial Cu^I/PMDETA complex.

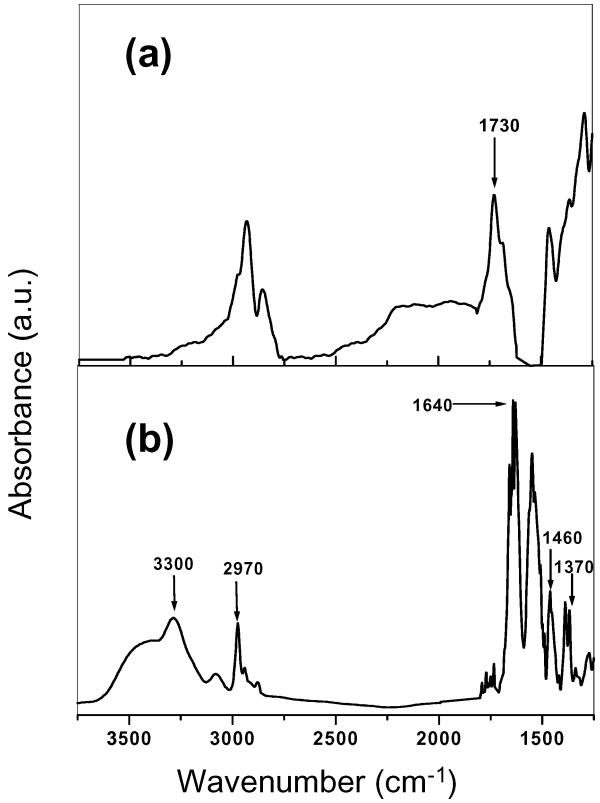

Figure 1. Reflectance FTIR spectra of (a) a thiol initiator monolayer on gold and (b) a pNIPAAM brush grown by surface-initiated polymerization on gold.

The polymerization of acrylamide monomers is more complicated than that of other vinyl monomers because of the possible complexation of the copper catalyst with the amide functionality of the growing polymer. This potential side reaction leads to uncontrolled polymerization,[50,51] lowers conversion, and limits brush growth. Recently, Matyjaszewski et al.[52] reported an increase in polymerization rate for 4-vinylpyridine when the ligand to catalyst molar ratio was increased from 1:1 to 6:1. To suppress competitive coordination of pNIPAAM to copper, we made use of this acceleration strategy, using a PMDETA to CuBr molar ratio of 5:1, to obtain high conversion of monomer. We choose PMDETA, which is a strong complexing ligand, because the coordination complex that forms between copper and simple amines has a relatively small redox potential.

(45) Hutter, J. L.; Bechhoefer, J. *Rev. Sci. Instrum.* **1993**, *64*, 1868−1873.
(46) Pan, Y. V.; Wesley, R. A.; Luginbuhl, R.; Denton, D. D.; Ratner, B. D. *Biomacromolecules* **2001**, *2*, 32−36.
(47) Wang, X. S.; Lascelles, S. F.; Jackson, R. A.; Armes, S. P. *Chem. Commun.* **1999**, 1817−1818.
(48) Wang, X. S.; Armes, S. P. *Macromolecules* **2000**, *33*, 6640−6647.
(49) Matsuo, E. S.; Orkisz, M.; Sun, S. T.; Li, Y.; Tanaka, T. *Macromolecules* **1994**, *27*, 6791−6796.
(50) Teodorescu, M.; Matyjaszewski, K. *Macromolecules* **1999**, *32*, 4826−4831.
(51) Rademacher, J. T.; Baum, R.; Pallack, M. E.; Brittain, W. J.; Simonsick, W. J. *Macromolecules* **2000**, *33*, 284−288.
(52) Xia, J. H.; Zhang, X.; Matyjaszewski, K. *Macromolecules* **1999**, *32*, 3531−3533.

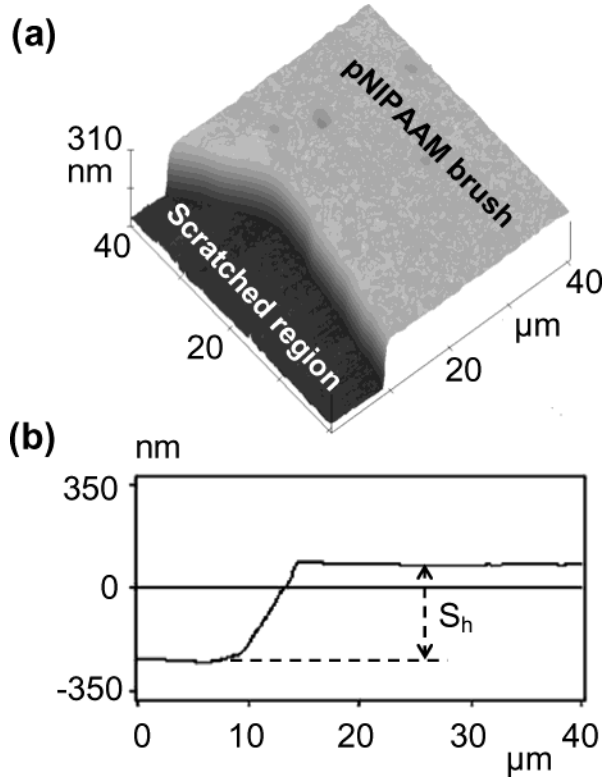

Figure 2. pNIPAAM brush grown by surface-initiated polymerization on gold after 60 min of reaction time: (a) three-dimensional AFM height image (contact mode in air at 25 °C) and (b) corresponding average cross-section. The average brush thickness (B_t) is 253 nm in air, and the RMS roughness over a 20 μm × 20 μm area is 6.1 nm. The brush height was obtained by averaged cross-sectional analysis of the AFM height image taken on a region of the sample where part of the brush and the underlying gold and chromium layer of known thickness have been removed.

The effective amount of initiator immobilized on the surface in surface-initiated ATRP is small so that only a low concentration of catalyst Cu(I) is needed to maintain rapid brush growth.[53] We chose to work with a catalyst concentration of about 0.44 mM, which corresponds to a molar ratio of NIPAAM monomer (1.9 M) to Cu(I) of 4300:1, an amount that was still enough for surface-initiated polymerization but that also decreased the steady-state radical concentration sufficiently to minimize bimolecular termination reactions. This catalyst concentration, however, is significantly lower (approximately 45 times less) than that reported by others.[29,30] At this ratio, a pNIPAAM brush can be polymerized with a thickness of about 250 nm (dry state) in 1 h of reaction time (Figures 2 and 3). A detailed analysis of the catalyst concentration on pNIPAAM brush growth is currently under way.

We measured the thickness of pNIPAAM brushes in air by cross-sectional analysis of AFM contact mode height images (Figure 2) and by ellipsometry. The brush thicknesses obtained from ellipsometry and from AFM height images are different; this difference can be explained by realizing that, in contrast to AFM height measurements, ellipsometry yields an optical thickness that is averaged over a large area (on the order of mm^2).

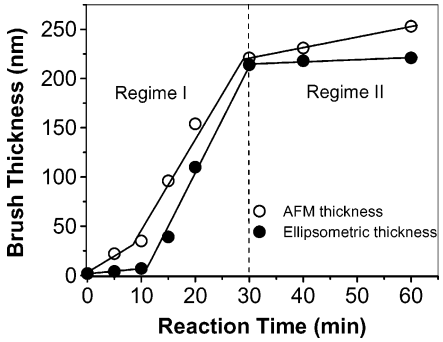

Figure 3. Average pNIPAAM dry brush height in air plotted as a function of polymerization time, measured by AFM (open circles) and ellipsometry (filled circles). The standard deviations of brush height on at least three different spots were less than 20% when measured by AFM and less than 15% when measured by ellipsometry for all the substrates. Each data point represents a measurement on a different substrate.

AFM contact mode height images revealed that the polymer brushes are smooth and homogeneous; for example, a 253 nm thick brush in the dry state had a root-mean-squared (RMS) roughness of less than 6.5 nm over a 20 μm × 20 μm area.

Although the measured AFM brush thickness in aqueous media depends on the applied imaging force below the LCST, we found that it is largely unaffected by the applied imaging force above the LCST, suggesting a considerable stiffening of the brush in its collapsed state.[43] When dry brush thickness is plotted as a function of polymerization time (Figure 3), the AFM and ellipsometric thicknesses show that brush growth occurs in two regimes. In regime I ($0 < t < 30$ min), growth is nonlinear, and in regime II ($t > 30$ min) the growth rate declines sharply. The nonlinear behavior in regime I suggests that brush growth is likely uncontrolled since no deactivator ($CuBr_2$) was present in the reaction mixture. The loss of growth rate in regime II possibly results from growing chains that become buried within the film and thus become inaccessible to monomers, which ultimately limits surface-initiated polymerization. Another possibility to explain the stagnant growth is the deactivation of the catalyst by forming a competitive complex with growing poly(*N*-isopropylacrylamide), similar to that previously reported for the polymerization of (meth)acrylamides using linear amines.[50,51]

Phase Behavior and Mechanical Characterization. The interesting phase behavior of pNIPAAM in solution reflects the balance of like and unlike interactions among its own segments and the surrounding solvent molecules. The inverse solubility upon heating of pNIPAAM in solution likely arises from changes in the number or strength of hydrogen bonds that develop between the solvent and polar groups on the polymer, as water molecules must reorient around nonpolar regions on the polymer backbone, having no opportunity to hydrogen bond there.[31]

In addition to temperature, cosolvents can cause an inverse phase transition in pNIPAAM. The addition of methanol to aqueous pNIPAAM solutions in the range from 10 to 65 vol % leads to co-nonsolvency,[32,33,54] effectively shifting the LCST of pNIPAAM in solution

(53) Kim, J. B.; Huang, W. X.; Miller, M. D.; Baker, G. L.; Bruening, M. L. *J. Polym. Sci., A: Polym. Chem.* **2003**, *41*, 386−394.

(54) Winnik, F. M.; Ottaviani, M. F.; Bossmann, S. H.; Garciagaribay, M.; Turro, N. J. *Macromolecules* **1992**, *25*, 6007−6017.

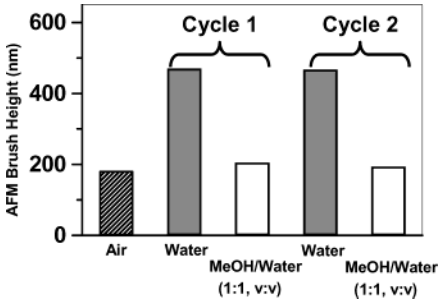

Figure 4. pNIPAAM brush thickness (25 min reaction time) plotted as a function of the solvent conditions (AFM height measurement). Key: brush in air (patterned bar; brush collapsed) and after cyclic exposure (two cycles) to first Milli-Q-grade water (gray bars; brush swollen) and then to a 1:1 (v/v) MeOH/water mixture (white bars; brush collapsed).

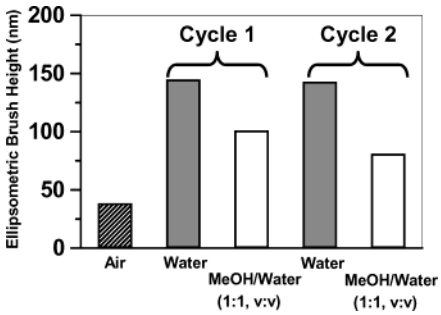

Figure 5. pNIPAAM brush thickness (15 min reaction time) plotted as a function of the solvent conditions (ellipsometric measurement). Key: brush in air (patterned bar; brush collapsed) and after cyclic exposure (two cycles) to first Milli-Q-grade water (gray bars; brush swollen) and then to a 1:1 (v/v) MeOH/water mixture (white bars; brush collapsed).

to lower temperatures. For example, addition of 50% methanol by volume to aqueous pNIPAAM solutions lowers the LCST of pNIPAAM to below 0 °C. Increasing the methanol concentration to above 65% causes a dramatic increase in the LCST to values greater than that in pure water. Below the LCST, pNIPAAM is hydrated and the chains are in an expanded conformation. Above the LCST, pNIPAAM is in a hydrophobically collapsed conformational state.

We studied the reversible conformational mechanics of two different pNIPAAM brushes with AFM (Figure 4) and ellipsometry (Figure 5), using solvent swelling experiments. The data in Figures 4 and 5 show that a pNIPAAM brush in the dry, collapsed state swells significantly when exposed to water at room temperature; the brush thickness increased 2.6 times (AFM measurement) and 3.8 times (ellipsometric measurement) for the samples in Figures 4 and 5, respectively. As discussed above, the brushes are also responsive to the solvent composition. In pure water, the pNIPAAM brushes are in a good solvent at temperatures below the LCST and the brush is likely in an extended conformational state. After exposure to a water/MeOH (1:1, v/v) mixture, a poor solvent, the brush adopts a collapsed conformation at room temperature. The corresponding brush thickness decreased 2.3 times (AFM measurement) and 1.4 times (ellipsometric measurement) for the samples in Figures 4 and 5, respectively. We demonstrate the reversibility of these conformational changes through inverse transition cycling by repeatedly exposing the brush to water and water/MeOH (Figures 4 and 5). The ellipsometric brush thickness measurements (Figure 5) revealed that the conformational collapse in the second cycle was larger than the first collapse, suggesting that the fully collapsed state is not reached immediately. This difference is likely not associated with insufficient equilibration time between solvent changes as ellipsometric measurements of brush height were carried out such that the ellipsometric angles Ψ and Δ reached a reasonably constant value before the solvent conditions were switched. Interestingly, the brush thickness in the expanded conformational state was constant and unaffected by repeated cycles. The AFM brush thickness measurements did not reveal such a dependence on cycle number, likely because, in contrast to ellipsometry, AFM height measurements involve a direct, mechanical compression of the brush during imaging, rendering the measurements relatively insensitive to subtle conformational changes in the brush. While stimulus-responsive polymer networks typically shrink in all three dimensions simultaneously,[55] shrinkage in surface-confined polymer brushes is much less because the mobility of polymer chains is restricted largely to one dimension perpendicular to the substrate.[24,56]

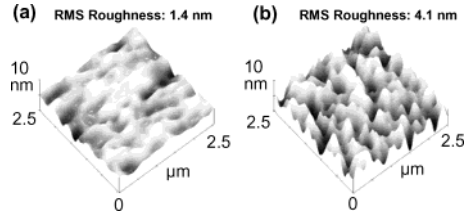

Figure 6. Three-dimensional AFM contact mode height images for a pNIPAAM brush (25 min reaction time) in (a) water and (b) a mixture of MeOH/water (1:1, v/v), showing a significant difference in surface roughness (RMS roughness 1.4 nm in water, RMS roughness 4.1 nm in the MeOH/water mixture).

The inverse phase transition affected not only brush thickness, but also brush surface morphology. The three-dimensional AFM surface plots (Figure 6) show that the brush is considerably smoother in water (RMS roughness ~1.4 nm within an area of 2.5 μm × 2.5 μm) than in a mixture of water/MeOH (1:1, v/v) (RMS roughness ~4.1 nm). The larger RMS roughness in the water/MeOH (1:1, v/v) mixture suggests the existence of domains that consist of aggregated collapsed polymer chains from which the solvent has been "excluded".

Surface Force Measurements. We performed AFM surface force measurements on surface-immobilized pNIPAAm brushes (5 and 60 min polymerization time on the substrate and cantilever, respectively) below and above the LCST to directly probe the effect of the phase transition on adhesion and polymer conformation. The measurement configuration and the solvent-dependent pNIPAAM conformations are illustrated schematically in the insets to Figure 7. When two polymer-bearing surfaces are brought into increasingly compressive contact, repulsive steric forces arise from the restriction of conformational degrees of freedom of the thermally mobile polymer chains. The repulsive force contribution

(55) Shibayama, M.; Tanaka, T. *Adv. Polym. Sci.* **1993**, *109*, 1−62.
(56) Dingenouts, N.; Norhausen, C.; Ballauff, M. *Macromolecules* **1998**, *31*, 8912−8917.

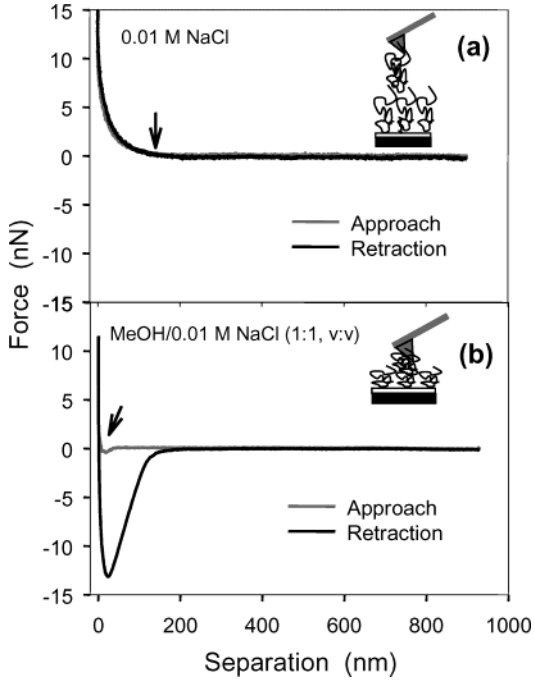

Figure 7. Typical force−separation profiles for a pNIPAAM brush (5 min reaction time) and a pNIPAAM-decorated cantilever tip (60 min reaction time) interacting in (a) 0.01 M NaCl and (b) a mixture of MeOH/0.01 M NaCl (1:1, v/v). The arrows indicate the onset of repulsive force interactions for each case. The insets illustrate schematically the experimental configuration.

due to electric double-layer overlap is expected to be small and of short range ($\kappa^{-1} \leq 3$ nm), as experiments were performed in a background of 0.01 M NaCl. The separation distance, D, between the bare sample surface and the bare cantilever tip was calculated by letting the constant compliance region—the region at which the stiffness of the compressed polymer layers exceeds the spring constant of the cantilever—coincide with $D = 0$. This means that D could be in error up to the combined thickness of the surface- and tip-immobilized, highly compressed pNIPAAM brush. Assuming a tip radius of 100 nm, we estimate the interaction energy per unit area in the constant compliance regime at 10 nN of applied force to be on the order of 0.1 N/m. This corresponds to a pressure on the brush that is significantly greater than that reported for other brush compressibility studies using AFM[44] or the surface force apparatus,[57,58] and we assume that at these pressures the brush is strongly compressed and the error in D is likely small.

Figure 7a shows that the interaction upon approach and retraction was monotonically repulsive below the LCST (0.01 M NaCl) and that the onset of steric interactions occurred at about 150 nm. From this interaction distance and the measured brush thickness on the sample substrate of about 60 nm (in the water-swollen state), we estimate the unknown brush height on the AFM cantilever tip to be about 90 nm. We find (unpublished results) that brush growth becomes limited when the brush height is on the order of the lateral feature size of the initiator patch, and this observation

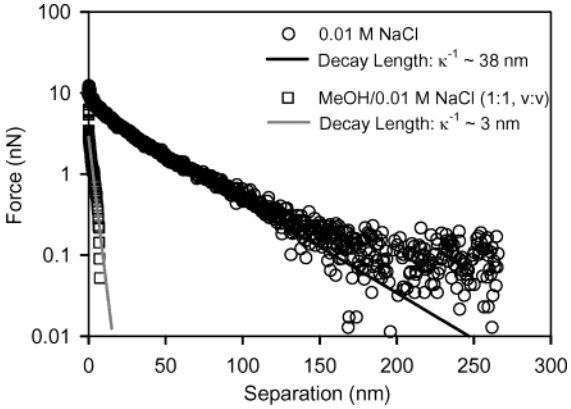

Figure 8. Force on approach (data from Figure 7) in 0.01 M NaCl (open circles) and a 1:1 (v/v) MeOH/0.01 M NaCl mixture (open squares) plotted as a function of separation and fitted to a decaying exponential function (semilogarithmic plot). The significant change in polymer conformation associated with the collapse of the polymer brush during a phase transition can be inferred from the decrease in decay length, κ^{-1}, from about 38 to about 3 nm.

likely explains why the brush thickness on the cantilever tip is less than that found for flat substrates after a 60 min polymerization time. Figure 7b shows that the force upon approach in the water/MeOH mixture goes through a small attractive minimum, followed by a significantly reduced steric repulsion regime when compared to the interaction in water alone, and that upon retraction a large unspecific adhesion force occurs. These observations suggest that in the water/MeOH mixture the pNIPAAm brush is in a hydrophobically collapsed state. The force minimum on approach likely arises from attractive polymer−segment interactions, whose number increases with increasing compression of the brush surfaces until, with further compression, the restriction in conformational degrees of freedom finally dominates and gives rise to strong, steric repulsive forces.

The significant change in polymer conformation associated with the collapse of the polymer brush during a phase transition can be inferred from the decrease in decay length, κ^{-1}, from about 38 to about 3 nm, obtained by fitting to an inverse exponential function (eq 2), where F is the force and D is the separation distance (Figure 8).

$$F(D) \propto e^{-\kappa D} \tag{2}$$

We also measured the reversible change in surface energy associated with a phase transition by measuring "pull-off" forces (i.e., the maximum force required to liberate the cantilever from surface contact). These forces are a good measure of adhesion, and thus surface energy, as they do not contain contributions from elastic surface deformation.[59] There was no adhesion between the polymer brushes in water (0.01 M NaCl) alone (Figure 7a). In the MeOH/water mixture the average adhesion force between pNIPAAM brushes was on the order of 12 nN (Figure 7b). The adhesion force distributions obtained from many ($n = 150$) approach−retraction cycles in water and in MeOH/water are shown in

(57) Klein, J.; Luckham, P. F. *Macromolecules* **1984**, *17*, 1041−1048.
(58) Luckham, P. F.; Klein, J. *Macromolecules* **1985**, *18*, 721−728.
(59) Lemieux, M.; Minko, S.; Usov, D.; Stamm, M.; Tsukruk, V. V. *Langmuir* **2003**, *19*, 6126−6134.

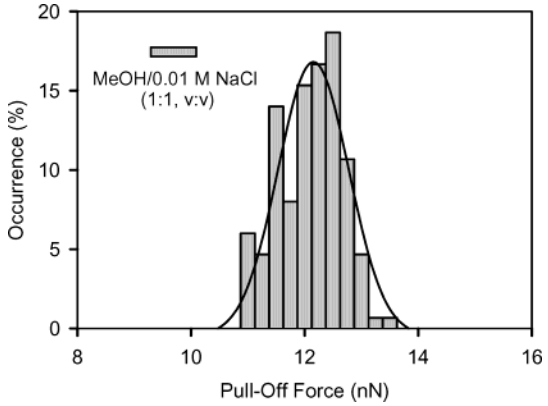

Figure 9. Adhesion force distributions for the interaction of a pNIPAAM brush (5 min reaction time) and a pNIPAAM-decorated cantilever tip (60 min reaction time) in a mixture of MeOH/0.01 M NaCl (1:1, v/v). The interactions in 0.01M NaCl were always repulsive. The data reflect a total of 150 approach−retraction cycles on different locations of the sample.

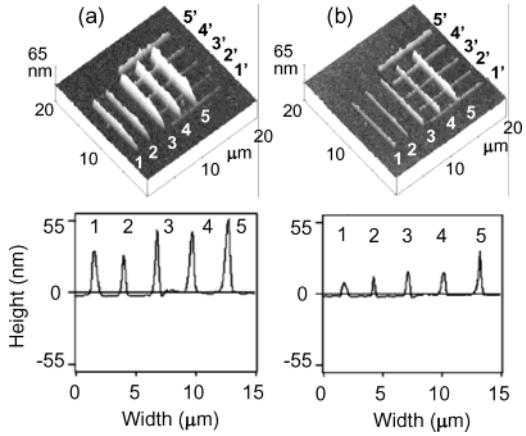

Figure 10. Contact mode AFM height images (20 μm × 20 μm) and corresponding typical height profiles of a pNIPAAM brush line nanopattern (60 min reaction time) imaged at room temperature in (a) Milli-Q-grade water and (b) a mixture of MeOH/water (1:1, v/v). The pNIPAAM line pattern was generated by first removing a thiol resist through nanoshaving under large normal forces (∼50 nN) using an atomic force microscope and subsequent surface-initiated polymerization of NIPAAM for 60 min using a backfilled, covalently attached thiol initiator (**1**). The line number corresponds to the nanoshaving time of a line in minutes. Reprinted from ref 24. Copyright 2004 American Chemical Society.

Figure 9. This adhesion likely arises from van der Waals forces that can effectively act between the hydrophobically collapsed polymer segments on the substrate and tip.[60] The reversibility of these adhesion forces was demonstrated for three solvent exchange cycles, where essentially the same adhesion force distributions were obtained in each of the three cycles, suggesting that the effect of a phase transition on the surface energy (adhesion) is entirely reversible (data not shown).

Nanopatterning. Figure 10 shows a typical pNIPAAM brush line pattern with line widths of about 500 nm and line lengths of about 10 μm, imaged in (a) water and (b) a mixture of water/MeOH (1:1, v/v). The AFM topographic images were collected in contact mode while scanning was done laterally (scan angle 90°) over

(60) Schmitt, F.-J.; Park, C.; Simon, J.; Ringsdorf, H.; Israelachvili, J. *Langmuir* **1998**, *14*, 2838−2845.

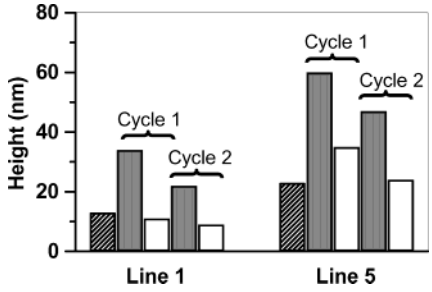

Figure 11. Average line height plotted for the pNIPAAM brush lines labeled 1 and 5 in Figure 10 as a function of the solvent conditions. Key: brush in air (patterned bar; brush collapsed) and after cyclic exposure (two cycles) to first Milli-Q-grade water (gray bars; brush swollen) and then to a 1:1 (v/v) MeOH/water mixture (white bars; brush collapsed).

the lines labeled 1−5 (set 1). The set of lines labeled 1−5 (set 1) was patterned before the set of lines labeled 1′−5′ (set 2). The line number corresponds to the nanoshaving time in minutes. The polymer brush thickness obtained from averaged height profiles of lines 1−5 (set 1) in Figure 10 depend not only on the solvent (discussed below) but also on the nanoshaving conditions such as tip force and shaving time. The average line height for the patterned pNIPAAM brush lines labeled 1 and 5 in Figure 10 is plotted as a function of the solvent conditions in Figure 11. The data in Figure 11 show that the brush thickness increases with increasing shaving time (indicated in minutes directly by the line number) assuming that the shaving force remains approximately constant while the lines of set 1 are shaved. For example, the average heights of line 1 (1 min of shaving) are 13, 34, and 11 nm in air, water, and a mixture of water/MeOH (1:1, v/v), respectively. In the case of line 5 (5 min of shaving), the corresponding heights are 23, 60, and 35 nm. This dependence of the brush thickness on shaving time is likely associated with the degree of resist removal, where at short shaving times the number of residual thiol resist molecules is larger than that at long shaving times. The degree of resist removal will directly affect the initiator surface density that can be achieved by backfilling. The brush thickness is a function of the initiator surface density, where low initiator densities lead to low brush thicknesses. This was recently shown by Huck et al.,[37] where SAMs containing 10% and 50% thiol initiator **1** grew poly(methyl methacrylate) (PMMA) brushes to approximately 1/10 and 1/2 the thickness of PMMA brushes initiated from SAMs comprising 100% thiol initiator. The apparent brush thicknesses of the patterned brushes were significantly smaller, at equal reaction times, when compared with those of bulk pNIPAAM brushes likely due to immobilization of different initiator surface densities.

The line pattern in Figure 10 and the data in Figure 11 also show that the conformation of nanopatterned pNIPAAM brushes is significantly affected by the solvent conditions. When exposed to water at room temperature, dry pNIPAAM brushes swell considerably and more than double their thickness. pNIPAAM brushes are also responsive to the solvent composition. For example, in pure water and at temperatures below the LCST, pNIPAAM brushes are in a good solvent and adopt an extended conformation. After exposure to a

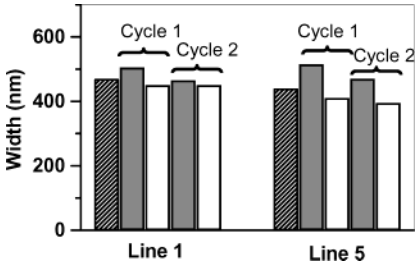

Figure 12. Average line width plotted for the pNIPAAM brush lines labeled 1 and 5 in Figure 11 as a function of the solvent conditions. Key: brush in air (patterned bar; brush collapsed) and after cyclic exposure (two cycles) to first Milli-Q-grade water (gray bars; brush swollen) and then to a 1:1 (v/v) MeOH/water mixture (white bars; brush collapsed).

water/MeOH (1:1, v/v) mixture (poor solvent), the brushes adopt a hydrophobically collapsed conformation.[32,33] We demonstrated the reversibility of this stimulus-responsive conformational change of nanopatterned brushes by cyclic exposure to water and water/methanol mixtures (1:1, v/v) (inverse transition cycling).

Figure 11 shows that the average heights of, for example, lines 1 and 5 decrease after addition of 50% (v) MeOH as a cosolvent to pure water, by 3.1 times and 1.7 times, respectively. In a second transition cycle the original brush line heights were not completely recovered (Figure 11). This may be due to an incomplete rehydration of the brush in the experimental time frame. Figure 10 shows that a second set of lines labeled 1′−5′ (set 2), oriented perpendicularly to lines 1−5 of set 1, have smaller feature heights and appear not to be as responsive to the solvent conditions as the lines of set 1, although the shaving times for the lines in set 1 and in set 2 were the same. The perceived lack of responsiveness for the lines in set 2 is in part due to the chosen out-of-plane scaling.[24] We attribute the smaller feature heights of the lines in set 2 to overall smaller shaving forces, as the lines of set 2 were shaved after all lines in set 1 had been completed. It is likely that the applied nanoshaving forces at the time of shaving the lines from set 2 were diminished due to drift in the cantilever deflection set point of the atomic force microscope. Small shaving forces lead to less efficient removal of the thiol resist, ultimately again lowering the surface density of initiator **1**.

Figure 12 shows that the averaged widths of the pNIPAAM line patterns are affected only slightly by the solvent conditions. The line widths are slightly smaller in air and in the water/MeOH mixture (1:1, v/v) when compared with the widths in pure water. Our findings are thus consistent with the expected behavior of laterally confined and covalently attached stimulus-responsive polymer chains, where the average chain height can be affected significantly by application of external stimuli because the chain mobility is largely restricted to one dimension perpendicular to the substrate.[56]

We were able to fabricate polymer brush nanopatterns with an aspect ratio (height:width) of about 1:10 in an extended state, and we expect that further improvements in the nanoshaving process such as the use of sharpened probe tips, closed-loop position control of the XY-scanner, and careful control of the shaving conditions, such as speed and applied force, will result in considerably reduced feature dimensions.

Conclusions

We have demonstrated the surface-initiated polymerization of stimulus-responsive pNIPAAM brushes from monolayers of **1** on gold-coated surfaces. Our polymerization conditions differ from those of previous approaches in that NIPAAM was polymerized in water at a low methanol concentration and a low catalyst to monomer ratio at room temperature. By adopting low methanol concentrations during polymerization, the growing pNIPAAM chains were maintained in a hydrophilic and an extended conformational state, yielding thick polymer brush layers.

In addition, we have presented the prototypical fabrication of nanopatterned, surface-confined, stimulus-responsive pNIPAAM brushes in a grafting-from approach using a simple strategy that combines nanoshaving, an SPL method, with surface-initiated polymerization.[24] The reversible, stimulus-responsive conformational height change of these bulk and nanopatterned polymer brushes is consistent with the behavior of surface-confined polymer chains, where chain mobility is restricted largely to one dimension perpendicular to the substrate. The polymerization and patterning approach is generic and can likely be extended to a wide variety of monomers.

Acknowledgment. We thank the National Science Foundation for support through Grants NSF EEC-021059, NSF DMR-0239769 CAREER AWARD, and ARO DAADG55-98-D-0002. We thank Dr. Tommy Nylander and Yulia Samoshina (Department of Physical Chemistry I, Lund University, Sweden) for their generous help with the ellipsometric measurements.

CM049562Y